The Journal of Immunology
RESEARCH ARTICLE | JANUARY 01 2009

Reciprocal Expression and Signaling of TLR4 and TLR9 in the Pathogenesis and Treatment of Necrotizing Enterocolitis[1]

Steven C. Gribar; ... et. al

J Immunol (2009) 182 (1): 636–646.
https://doi.org/10.4049/jimmunol.182.1.636

Reciprocal Expression and Signaling of TLR4 and TLR9 in the Pathogenesis and Treatment of Necrotizing Enterocolitis[1]

Steven C. Gribar, Chhinder P. Sodhi, Ward M. Richardson, Rahul J. Anand, George K. Gittes, Maria F. Branca, Adam Jakub, Xia-hua Shi, Sohail Shah, John A. Ozolek, and David J. Hackam[2]

Necrotizing enterocolitis (NEC) is a common and often fatal inflammatory disorder affecting preterm infants that develops upon interaction of indigenous bacteria with the premature intestine. We now demonstrate that the developing mouse intestine shows reciprocal patterns of expression of TLR4 and TLR9, the receptor for bacterial DNA (CpG-DNA). Using a novel ultrasound-guided in utero injection system, we administered LPS directly into the stomachs of early and late gestation fetuses to induce TLR4 signaling and demonstrated that TLR4-mediated signaling within the developing intestine follows its expression pattern. Murine and human NEC were associated with increased intestinal TLR4 and decreased TLR9 expression, suggesting that reciprocal TLR4 and TLR9 signaling may occur in the pathogenesis of NEC. Enteral administration of adenovirus expressing mutant TLR4 to neonatal mice reduced the severity of NEC and increased TLR9 expression within the intestine. Activation of TLR9 with CpG-DNA inhibited LPS-mediated TLR4 signaling in enterocytes in a mechanism dependent upon the inhibitory molecule IRAK-M. Strikingly, TLR9 activation with CpG-DNA significantly reduced NEC severity, whereas TLR9-deficient mice exhibited increased NEC severity. Thus, the reciprocal nature of TLR4 and TLR9 signaling within the neonatal intestine plays a role in the development of NEC and provides novel therapeutic approaches to this disease. ***The Journal of Immunology,*** **2009, 182: 636–646.**

Necrotizing enterocolitis (NEC)[3] is the leading cause of death from gastrointestinal disease in preterm infants and is characterized by the development of intestinal necrosis, systemic sepsis, and multisystem organ failure (1, 2). Although the mechanisms that lead to the development of NEC remain incompletely understood, several lines of evidence point to a critical role for the interaction between indigenous bacteria and the newborn intestine in its pathogenesis (3, 4). LPS, a glycolipid component of the outer membrane of Gram-negative bacteria, is one of the most abundant proinflammatory stimuli in the gastrointestinal tract (5, 6) and activates the innate immune receptor TLR4 within the intestine (7). We and others have shown that TLR4 activation by LPS adversely affects the enterocyte monolayer through increased apoptosis (8, 9) and impairs mucosal healing through reduced enterocyte proliferation and migration (8). These factors lead to the translocation of bacteria across the intestinal monolayer, a process that we have shown to be mediated in part by the TLR4-dependent internalization of bacteria by enterocytes (10). We and others have demonstrated a direct role for TLR4 in the pathogenesis of NEC, as mice with inhibitory mutations in TLR4 are protected from the development of NEC through salutary effects on intestinal injury and repair (8, 11). Taken together, these findings indicate that activation of TLR4 by LPS plays an important role in the pathogenesis of NEC through its effects in the disruption of the enterocyte monolayer and that strategies that limit the responsiveness of the intestine to LPS may provide a therapeutic approach to the management of this disease.

In addition to expressing high concentrations of LPS, it is noteworthy that bacteria within the intestinal lumen are rich in DNA. Bacterial DNA differs from mammalian DNA in that it is both enriched with CpG motifs and largely demethylated compared with mammalian DNA (12) and, as such, is recognized by a unique signaling receptor, TLR9 (13). Although TLR9 activation leads to enhanced proinflammatory cytokine release from macrophages (14), TLR9 activation with CpG-DNA has recently been shown to limit the extent of experimental colonic inflammation through pathways that remain incompletely understood (15); however, a role for TLR9 in the pathogenesis of NEC remains unexplored. Moreover, the pattern of expression of TLR4 and TLR9 in the developing intestine, the signaling capacity of TLR4 during intestinal development, and the expression of TLR4 and TLR9 in the postnatal, premature gut remains unknown. Importantly, such information may provide important insights into the pathogenesis of NEC and explain why its development appears to be restricted to preterm infants.

In seeking to understand the increased susceptibility of the preterm infant to the development of NEC, we now focus on the expression of TLR4 and TLR9 within the developing intestine and examine the relative roles of TLR4 and TLR9 signaling in the neonatal intestinal inflammatory response. We now provide evidence that NEC develops in the setting of reduced TLR9 expression and increased TLR4 expression in the developing intestinal mucosa, that intestinal TLR4 expression is functionally active during development, that TLR4 signaling in enterocytes plays a

Department of Surgery, Division of Pediatric Surgery, Children's Hospital of Pittsburgh and Department of Pathology, Division of Pediatric Pathology, University of Pittsburgh School of Medicine, Pittsburgh, PA 15213

Received for publication August 11, 2008. Accepted for publication October 22, 2008.

The costs of publication of this article were defrayed in part by the payment of page charges. This article must therefore be hereby marked *advertisement* in accordance with 18 U.S.C. Section 1734 solely to indicate this fact.

[1] This work was supported by National Institutes of Health Grant 1R01-GM078238-01 (to D.J.H.). S.C.G. and W.M.R. are supported in part by the Loan Repayment Program for Pediatric Research of the National Institutes of Health. S.C.G. is supported by the American College of Surgeons Research Fellowship. W.M.R. is supported by the Surgical Infection Society Resident Research Award.

[2] Address correspondence and reprint requests to Dr. David J. Hackam, Division of Pediatric Surgery, Room 4A-486 DeSoto Wing, Children's Hospital of Pittsburgh, Pittsburgh, PA 15213. E-mail address: david.hackam@chp.edu

[3] Abbreviations used in this paper: NEC, necrotizing enterocolitis; E, embryonic day; IRAK, IL-1R-associated kinase; ODN, oligodeoxynucleotide; siRNA, small interfering RNA; TRAF, TNFR-associated factor.

critical role in the development of NEC, and that activation of TLR9 with CpG-DNA inhibits TLR4-mediated signaling in enterocytes in a mechanism dependent upon the inhibitory signaling molecule IL-1R-associated kinase (IRAK) M (IRAK-M). Strikingly, activation of TLR9 in vivo with the administration of CpG-DNA to newborn mice was found to significantly reduce the incidence of experimental NEC through reduced enterocyte apoptosis and bacterial translocation. Taken together, these findings provide evidence that the reciprocal nature of TLR4 and TLR9 signaling within the neonatal intestine plays a role in the development of NEC and provides the possibility for novel therapeutic approaches to this devastating disorder.

Materials and Methods

Cell culture and reagents

IEC-6 enterocytes and J774 macrophages were obtained from the American Type Culture Collection and maintained as described (16, 17). Phosphorothioated CpG-DNA, oligodeoxynucleotide (ODN) 1826 (TCCAT GACGTTCCTGACGTT), and control GpC-DNA, control ODN 1826 (TCCATGAGCTTCCTGAGCTT), were synthesized by the University of Pittsburgh DNA synthesis facility. ODNs were confirmed to be endotoxin-free (<0.05 endotoxin U/ml) by *Limulus* assay. Abs were obtained as follows: TLR9 from Imgenex; NF-κB (p65 subunit), IRAK1, TLR9 (H-100) (immunohistochemistry), and TLR4 (L14) from Santa Cruz Biotechnology; IRAK-M Ab A from Sigma-Aldrich and Ab B from Chemicon; cleaved caspase-3, phospho-p38-MAPK, phospho-ERK, total p38-MAPK, and total ERK from Cell Signaling Technology; GM130 from BD Biosciences; TNFR-associated factor 6 (TRAF6) from Abcam; and LAMP-2 from Developmental Studies Hybridoma Bank, University of Iowa (Iowa City, IA). Appropriate secondary Abs for immunohistochemistry and SDS-PAGE were obtained from Molecular Probes and Jackson ImmunoResearch Laboratories, respectively, including Alexa Fluor 488 (green) and Cy3 (red).

For knockdown of TLR9 or IRAK-M, IEC-6 enterocytes were cultured in antibiotic-free medium and exposed to TLR9- or IRAK-M-specific ON-TARGETplus SMARTpool small interfering RNA (siRNA; 100 nM final concentration; Dharmacon) or negative control, nontargeted siRNA (100 nM final concentration; Dharmacon) for 48 h, at which time the cells were washed with PBS and medium changed to IEC-6 growth medium. After a period of 24 additional hours, cells were assessed for TLR9 expression by reverse transcriptase PCR or IRAK-M expression by Western blotting or used as described below.

Assessment of the ontogeny of expression of TLR4 and TLR9 in the developing intestine

Samples of the small intestine were harvested from prenatal or postnatal mice that were generated by timed mating (strain Swiss Webster), considering noon on the day that a vaginal plug was observed as 0.5 day postcoitum during different stages (embryonic day (E)14.5 to adult) of mouse gut development. The ileum was dissected from freshly harvested intestinal specimens using an Olympus SZ61stereomicroscope, and sections were obtained 1 cm proximal to the cecum. Intestinal sections were stabilized in RNAlater (Qiagen), and RNA was isolated using the RNeasy kit (Qiagen). One microgram of total RNA was reverse transcribed to cDNA and used for PCR amplification reactions with the real-time IQ5 thermal cycler system (Bio-Rad) as described in detail below.

In utero intraintestinal injections of early mouse embryos

To directly assess the signaling capability of TLR4 within the embryonic intestines, we used the following ultrasound-guided backscatter microscopy system. This system allows for the visualization of early mouse embryos after a laparotomy on the mother and delivery of an individual uterine saccule through a fenestration into a saline-filled petri dish. Once positioned, a 30-μm glass syringe containing either saline or fluorescein-labeled LPS (5 μl of 1 mg/ml stock; Invitrogen) was introduced under direct vision into the intestine and the contents were delivered. Animals were sacrificed 3 h later, and the success of injection was determined by assessing the presence of fluorescein dye within the lumen of the intestine under standard filter sets on an Olympus SZX12 fluorescent microscope. The extent of TLR4-mediated signaling in the developing intestine was assessed by evaluating the intestinal expression of IL-6 using quantitative PCR (see below).

Generation of adenoviruses bearing wild-type and mutant TLR4

Replication-deficient recombinant adenoviruses that express GFP-tagged mouse TLR4-cDNA, as well as the control adenovirus that expresses only GFP, were prepared using the Adeno-X Expression System2 kit (Clontech). Briefly, the respective expression cassettes were cloned in-frame with loxP sites into a donor vector, verified for the correct ligation by RT-PCR and Western blot analysis, and transferred into the E1a genomic region of human type 5 adenovirus (Ad5) by Cre-loxP recombination. The resulting adenovirus constructs were propagated into a high-titer virus in permissive HEK 293 cells. The high-titer viruses were verified again by RT-PCR and Western blot analysis, as well for the multiplicity of infection.

To assess the adequacy of adenoviral GFP-mutant TLR4 to inhibit TLR4 signaling, IEC-6 cells were treated with viruses (GFP alone, wild-type TLR4, and mutant TLR4) 48 h before treatment with LPS (50 μg/ml; 1 h). Samples were assessed by SDS-PAGE for the expression of phospho-p38, and blots were stripped and reprobed for F-actin. In parallel, immortalized primary murine embryonic fibroblasts that express the NF-κB-inducible SEAP (secreted embryonic alkaline phosphatase) reporter gene (InvivoGen), and were isolated from 13 day old C3H/HeN (TLR4-wild type) embryos. TLR4-dependent activation of NF-κB drives the expression and secretion of SEAP in the supernatant, which was assayed using Quanti-Blue reagent (InvivoGen) in the presence of 15 μg/ml LPS using the Quanti-Blue system with measurements obtained at 630 nm using a Spectra Max plus plate reader (Molecular Devices).

Induction of endotoxemia and experimental necrotizing enterocolitis

All mice were housed and cared for at the Rangos Research Center, Children's Hospital of Pittsburgh (Pittsburgh, PA). All experiments were approved by the Children's Hospital of Pittsburgh Animal Care Committee and by the Institutional Review Board of the University of Pittsburgh. Swiss Webster (CFW) and C57BL/6 mice were obtained from The Jackson Laboratory; TLR9 mutant mice (CpG1) were provided by Dr. B. Beutler (The Scripps Research Institute, La Jolla, CA).

Endotoxemia was induced in 2-wk-old C57BL/6 (wild-type) or CpG1 (TLR9-mutant) mice by the i.p. injection of LPS (*Escherichia coli* 0111:B4 purified by gel filtration chromatography, >99% pure, 5 mg/kg; Sigma-Aldrich). In parallel, mice were administered vehicle (saline) or CpG-DNA (1 mg/kg). Three hours after injection, animals were sacrificed, and samples of the terminal ileum were obtained 1 cm proximal to the ileocecal valve and prepared as described below.

Experimental NEC was induced in mice as we have previously described and validated (8, 18). Briefly, 10- to 14-day-old mice (Swiss Webster, C57BL/6, or TLR9-mutant) were gavage fed (Similac advanced infant formula (Ross Pediatrics):Esbilac canine milk replacer at a ratio of 2:1) five times daily and exposed to intermittent hypoxia (5% O_2, 95% N_2) for 10 min using a modular hypoxic chamber (Billups-Rothenberg) twice daily for 4 days. Animals were fed 200 μl per 5 g of mouse body weight by gavage over 2–3 min using a 24-French angiocatheter that was placed into the mouse esophagus under direct vision. We and others have demonstrated that this experimental protocol induces intestinal inflammation and the release of proinflammatory cytokines in a pattern that closely resembles human NEC (11, 18–22). Control (i.e., non-NEC) animals remained with their mothers and received breast milk. Where indicated, breast fed animals of all strains were injected with CpG-DNA (1 mg/kg daily for 4 days) before sacrifice or exposed to hypoxia alone, or administered adenoviral GFP, GFP-wild-type TLR4, or GFP-mutant TLR4 twice daily for three days (240 μl; 10^{12} PFU). The expression of GFP in mucosal scrapings of the intestine, as well as the lung and liver, was assessed by RT-PCR as described below.

The severity of experimental NEC was graded by a pathologist blinded to the study groups and by an additional blinded observer using a previously validated scoring system from 0 (normal) to 3 (severe) as previously described (8, 21). Immediately after sacrifice, serum was obtained by retroorbital puncture and the terminal ileum was harvested 1 cm proximal to the ileocecal valve in 10% neutral buffered formalin or frozen in liquid nitrogen after embedding in Cryo-Gel (Cancer Diagnostics). Where indicated, mucosal scrapings were obtained by microdissection under ×20 power and collected in RNAlater (Qiagen).

Intestinal samples were obtained from human neonates undergoing intestinal resection for NEC or for unrelated indications (control). The intestinal mucosa was microdissected from the underlying submucosal tissue and placed in ice-cold tissue lysis buffer (10% glycerol, 62.5 mM Tris (pH 6.6), and 7.5% SDS) containing protease inhibitors (1 mM sodium pyrophosphate, 20 mM sodium fluoride, 2 μg/ml aprotinin, 5 μg/ml pepstatin, 0.5 mM PMSF, and 50 μM leupeptin) or placed in RNAlater solution. In

parallel, samples obtained at laparotomy from preterm human infants undergoing intestinal resection for management of NEC or at the time of stoma closure were either prepared for biochemical analysis (see below) or placed in 2% paraformaldehyde overnight, transferred to 30% sucrose, and then frozen in Cryo-Gel (Cancer Diagnostics) for immunohistochemical analysis (see below). All human tissue was obtained and processed as discarded tissue via waiver of consent with approval from the University of Pittsburgh Institutional Review Board and in accordance with the University of Pittsburgh anatomical tissue procurement guidelines.

Where indicated, resident peritoneal macrophages were obtained immediately after sacrifice from Swiss Webster mice using peritoneal lavage with 5 ml of ice-cold PBS as we have described (23). Cells were washed three times in PBS and then immediately stimulated with LPS (10 ng/ml) in the presence or absence of CpG-DNA (1 μM) for 1 h and subjected to SDS-PAGE or RT-PCR as described below.

Immunohistochemistry, immunofluorescence, and SDS-PAGE

The immunoanalysis of cultured enterocytes and mouse and human intestine was performed as previously described (18, 24) and evaluated using an Olympus FluoView 1000 confocal microscope under oil immersion objectives. Images were assembled using Adobe Photoshop CS2 software (Adobe Systems). In parallel, Cryo-Gel (Cancer Diagnostics) frozen sections of terminal ileum were sectioned (4 μm), rehydrated with PBS, and fixed with 2% paraformaldehyde. Nonspecific binding was blocked with 5% BSA. Sections were evaluated on an Olympus FluoView 1000 confocal microscope using oil immersion objectives as described above.

For assessment of NF-κB activation, IEC-6 enterocytes were treated with LPS (50 μg/ml, Sigma-Aldrich) and/or CpG-DNA (1 μM) either alone or in combination for 1 h and immunostained with Abs against the p65 subunit of NF-κB. This concentration of LPS was selected based upon the concentration of LPS that we measured in the stool of mice with experimental NEC and approximates that measured in human infants with this disorder (18). The extent of nuclear translocation was determined as described below. In brief, a threshold limit was set based upon the emission signal for the nuclear stain DRAQ5, which therefore defined a nuclear region of interest. To define a corresponding cytoplasmic region of interest, a circular region 12 pixels beyond the nucleus was stenciled upon each cell. The average integrated pixel intensity pertaining to the corresponding NF-κB emission within the cytoplasmic and nuclear regions was then determined for >200 cells per treatment group in at least four experiments per group using MetaMorph software version 6.1 (Molecular Devices).

Where indicated, the extent of apoptosis was quantified in vitro and in vivo as we have done previously (8) using the apoptosis marker cleaved caspase-3 and enumerating the number of caspase-3 positive cells as a percentage of the total number of cells present. At least 100 fields were assessed for each experimental group where indicated.

SDS-PAGE was performed as previously described (19). Blots were developed using the ECL reagent (ECL-Super Signal; Pierce) and developed on radiographic film.

Immunoprecipitation

IEC-6 enterocytes were plated on 100-mm dishes at ~80% confluence and treated with either LPS (50 μg/ml) in the presence or absence of CpG-DNA (1 μM) or CpG DNA (1 μM) alone for 2.5 min. After treatment, cells were immediately rinsed with PBS and lysed with cell lysis buffer (50 mM Tris-HCl containing 150 mM NaCl, 1% Triton X100, and protease inhibitors, pH 7.4). After centrifugation at 10,000 rpm for 10 min, the supernatant was subjected to immunoprecipitation. To precipitate IRAK1, 500 μg of cell lysate were mixed with 2 μg of anti-IRAK1 Ab and incubated at 4 °C overnight followed by incubation with protein A-/G-conjugated beads (Santa Cruz Biotechnology) at 4 C° for 2 h. The beads were washed four times with the cell lysis buffer and the proteins bound were released from the beads by boiling in SDS-PAGE sample buffer for 5 min. The samples were analyzed by SDS-PAGE and Western blotting as described above with Abs against IRAK1 and TRAF6.

Polymerase chain reaction

Quantitative real-time PCR in cultured enterocytes and intestinal tissue using the BioRad iCycler (Bio-Rad) was performed as previously described (8) with the following primer sequences: mouse IL-6, sense 5′-CCAATTTCCAATGCTCTCCT-3′ and antisense 5′-ACCACAGTGAG GAATGTCCA-3′ (182 bp); mouse iNOS sense 5′-CTGCTGGTGG TGACAAGCACATTT-3′, antisense 5′-ATGTCATGAGCAAAGGCG CAGAAC-3′ mouse TLR9, sense 5′-TATCCACCACCTGCACAACT-3′ and antisense 5′-TTCAGCTCCTCCAGTGTACG-3′ (165 bp). For studies in IEC-6 cells, the following rat primers were used: TLR9, sense 5′-CTACGCTTGTGTCTGGAGGA-3′ and antisense 5′-AGCA CAAACAGAGTCTTGCG-3′ (101 bp); rat β-actin, sense 5′-TTGCTGA CAGGATGCAGAAG-3′ and antisense 5′-CAGTGAGGCCAGGATA GAGC-3′ (145 bp). Primer sequences for GFP were as follows: sense 5′-AGAACGGCATCAAGGTGAAC-3′ and antisense 5′-TGCTCAGG TAGTGGTTGTCG-3′. Primer sequences for mouse TLR4 were forward 5′-TTTATTCAGAGCCGTTGGTG-3′ and reverse 5′-CAGAGGATT GTCCTCCCATT-3′. Gene expression was normalized to β-actin expression (mouse specific primer sequences: sense 5′-CCACAGCTGAGAGG GAAATC-3′ and antisense 5′-TCTCCAGGGAGGAAGAGGAT-3′

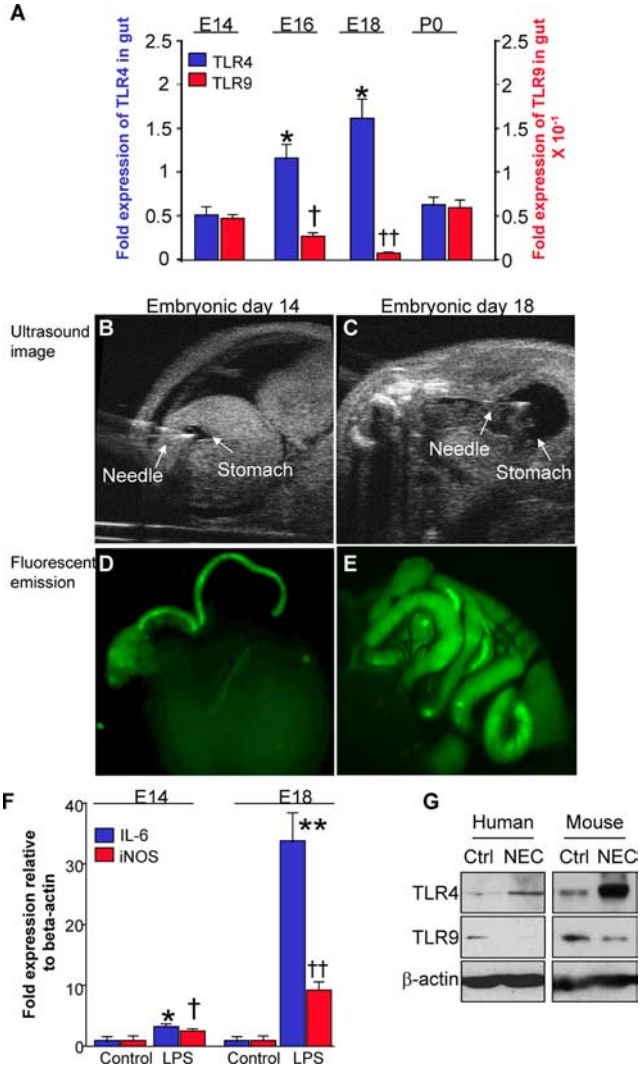

FIGURE 1. TLR4 and TLR9 are reciprocally expressed in the developing intestinal mucosa and in experimental and human NEC. *A*, Quantitative RT-PCR showing the expression relative to β-actin of TLR4 (blue) and TLR9 (red) in the intestine of Swiss Webster mice during gestation and in the postnatal period (P0) at the indicated times. Shown are mean and SEM from three separate experiments with 3 animals per group; *, $p < 0.05$ vs expression of TLR4 in E14 animals by ANOVA; †, $p < 0.05$ vs expression of TLR9 in E14 animals by ANOVA. *B–E*, Embryonic stomach was injected with fluorescein-labeled LPS (5 μl of 1 mg/ml solution) at E14 and E18 as described in *Materials and Methods* using ultrasound-guided backscatter microscopy. The ultrasound micrographs made during injection at E14 (*B*) and E18 (*C*) are shown in which the locations of the needle and stomach can be seen. Fluorescent emission of the harvested intestine at E14 (*D*) and E18 (*E*). *F*, Quantitative RT-PCR showing the expression of the proinflammatory cytokines IL-6 (blue) and inducible NO synthase (iNOS; red) in the intestine of mice that were injected with either LPS or saline (control) at E14 or E18 as shown. *G*, SDS-PAGE showing the expression of TLR4 and TLR9 in small intestinal mucosa obtained from healthy controls and patients or mice with NEC. Results shown are representative of four separate experiments. Ctrl, Control.

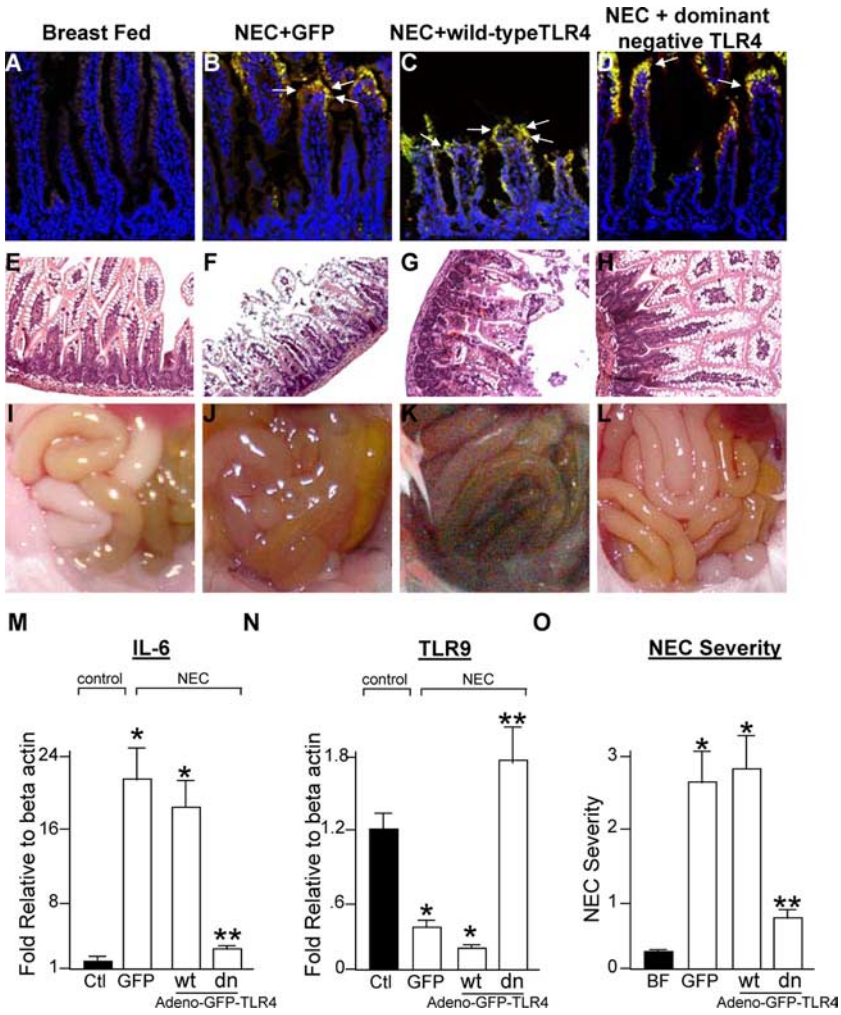

FIGURE 2. Adenoviral mediated inhibition of TLR4 signaling in enterocytes decreases intestinal inflammation in experimental NEC and increases the intestinal expression of TLR9. Ten-day-old mice were enterally administered GFP (*B*, *F*, and *J*), GFP-tagged wild-type TLR4 (*C*, *G*, and *K*), or GFP-tagged dominant negative TLR4 (all viruses: 240 μl,10^{12} PFU; *D*, *H*, and L) and were either breast fed (*A*, *E*, and *I*) or induced to develop experimental NEC. *A–D*, Sections of the terminal ileum from the indicated groups were immunostained for the expression of GFP, which was predominantly localized in the enterocytes (arrows). *E–H*, H&E staining of the architecture of the intestinal mucosa in the indicated groups. *I–L*, Gross appearance of the intestine immediately after sacrifice in breast-fed animals and those with experimental NEC that were administered the virus as indicated. *M* and *N*, RT-PCR showing the expression of the proinflammatory cytokine IL-6 (*M*) and TLR9 (*N*) in mucosal scrapings that were obtained from the intestine in breast fed mice (Ctl, Control) or those with experimental NEC that were administered the indicated viruses. *O*, Quantification of NEC severity in breast-fed (BF) animals (filled bars) or animals induced to develop experimental NEC along with the enteral coadministration of adenoviruses expressing GFP, GFP-tagged wild-type (wt) TLR4, or GFP-tagged dominant negative (dn) TLR4. *, $p < 0.05$ vs control or breast-fed animals by ANOVA; **, $p < 0.05$ vs wild-type TLR4 by ANOVA; three separate experiments.

(108 bp)). Where indicated, gene expression was assessed on 2.5% agarose gels using ethidium bromide staining. Images were obtained with a Kodak Gel Logic 100 imaging system using Kodak molecular imaging software.

Statistical analysis

Statistical analysis was performed using SPSS 13.0 software. ANOVA was used for comparisons in experiments involving more than two experimental groups. Two-tailed Student's *t* test was used for comparison for experiments consisting of two experimental groups. For analysis of the incidence of NEC, χ^2 analysis was performed.

Results

TLR4 and TLR9 are functional and are reciprocally expressed in the developing intestinal mucosa

To understand the potential role of the bacterial recognition receptors TLR4 and TLR9 in the development of intestinal inflammation in the neonate, we first explored the expression and function of these Toll-like receptors during intestinal development. To do so, we first harvested the intestines of mice at various time points during intestinal development and evaluated the intestinal expression of both TLR4 and TLR9 by RT-PCR. As shown in Fig. 1*A*, the intestinal expression of TLR4 increased from E14 to E18 and then decreased at term. By contrast, the expression of TLR9 decreased from E14 to E18 and then increased at term. These findings raise the possibility that alterations in the expression of TLR4 and TLR9 may influence the extent of LPS-mediated intestinal inflammation within the developing intestine, and we therefore next assessed the effects resulting from the unexpected exposure of the developing intestine to LPS. To do so, we used the novel backscatter in utero injection system described in *Materials and Methods*. Specifically, embryos were subjected to the intraintestinal injection of either saline or fluorescein-labeled LPS at either embryonic day 14 or embryonic day 18. A representative ultrasound image demonstrating the needle within the embryonic intestine at E14 and E18 is shown in Fig. 1, *B* and *C*, respectively. The fluorescent emission of the intestines that were harvested 3 h after injection reveals the presence of fluorescein dye throughout the intestine in fluorescein-LPS injected samples at E14 (Fig. 1*D*) and E18 (Fig. 1*E*). There was no detectable fluorescence in saline-injected samples (not shown). Importantly, the extent of LPS-mediated IL-6 expression within the developing intestine was significantly greater in an intestine injected at E18, in which TLR4 is high and TLR9 is low, than at E14 (Fig. 1*F*). It is also important to point out that at the time point at which TLR4 signaling was assessed, i.e., 3 h after injection, there was no change in the expression of TLR4 or TLR9 as compared with saline-injected samples (not shown). Taken together, these findings suggest that LPS-mediated IL-6 release may be in part influenced by the relative roles of TLR4 and TLR9 signaling within the intestine. Interestingly, both human and experimental NEC were associated with a relative increase in intestinal mucosal TLR4 expression and a decrease in TLR9 expression in the intestine (Fig. 1*G*). Together, these findings led us to explore the role, if any, of aberrant enterocyte TLR4 signaling in the development of NEC and the effects of TLR4 suppression using dominant negative

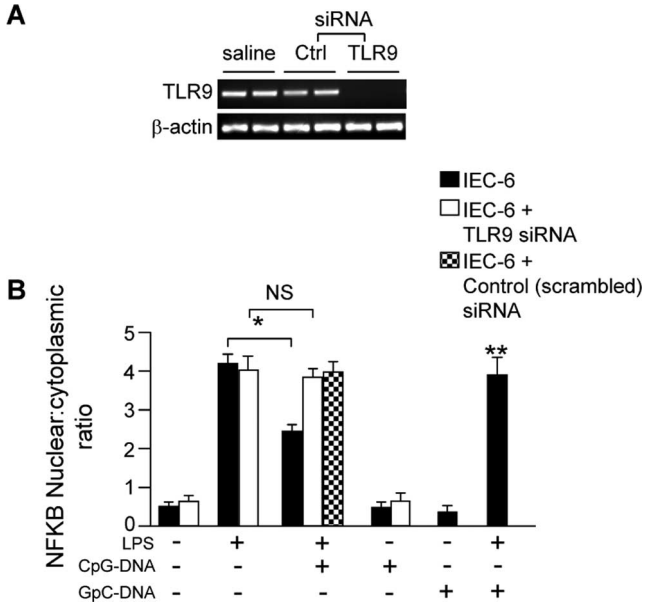

FIGURE 3. TLR9 activation reduces TLR4 signaling in IEC-6 cells enterocytes. *A*, RT-PCR showing TLR9 expression in IEC-6 cells that were treated with saline or siRNA (100 nM final concentration) against an unknown target (Ctrl, Control) or TLR9. The expression of β-actin in the same samples is shown. *B*, Quantification of the extent of NF-κB nuclear translocation as described in *Materials and Methods* for IEC-6 cells under the indicated conditions. Filled bars show effects in cells that were not treated with siRNA; open bars show cells treated with TLR9 siRNA; treatment with LPS (50 μg/ml) or CpG-DNA (1 μM) was for 1 h. Results are representative of five separate experiments with >100 cells per experiment; *, $p < 0.001$, ANOVA; **, $p < 0.05$, ANOVA vs untreated cells.

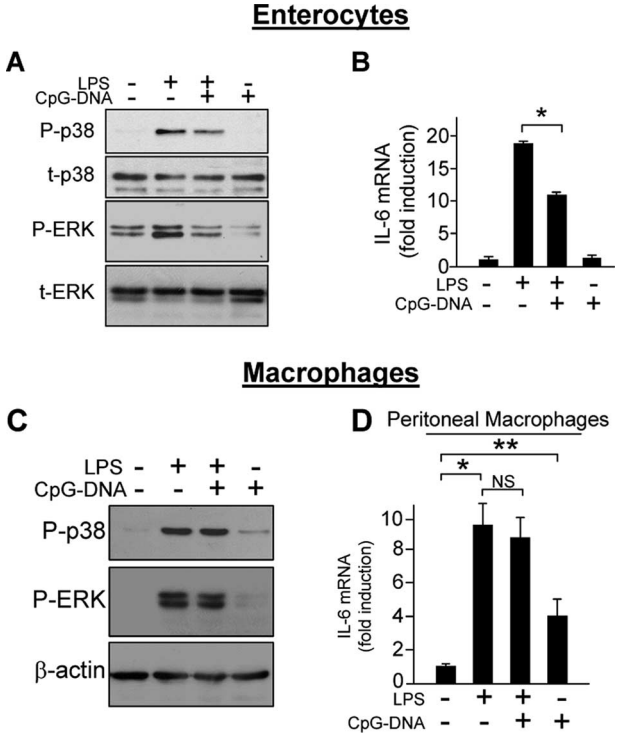

FIGURE 4. CpG-DNA attenuates TLR4 signaling in enterocytes but not in macrophages. *A*, SDS-PAGE showing expression of phospho-p38 (P-p38), total p38 (t-p38), phospho-ERK (P-ERK), and total ERK (t-ERK) in IEC-6 cells treated with LPS (50 μg/ml for 20 min) in the presence or absence of CpG-DNA (1 μM) as indicated. Blots were each probed with the indicated phospho-Ab and then stripped and reprobed with the indicated "total" Ab. *B*, RT-PCR showing the expression of IL-6 in IEC-6 cells under the indicated conditions. *, $p < 0.001$ by ANOVA. *C*, SDS-PAGE showing the expression of P-p38 and P-ERK in J774 macrophages in the presence or absence of LPS (10 ng/ml, 20 min) and CpG-DNA (1 μM). Blots were stripped and reprobed for β-actin. *D*, RT-PCR showing the expression of IL-6 in resident peritoneal macrophages in the presence or absence of LPS and CpG-DNA. Results shown are representative of three separate experiments. Shown are mean and SEM; *, $p = 0.009$; **, $p = 0.008$.

vectors or activators of TLR9 using CpG-DNA on TLR4-mediated signaling in enterocytes.

Adenoviral-mediated inhibition of TLR4 signaling in enterocytes decreases intestinal inflammation in experimental NEC and increases the intestinal expression of TLR9

We next sought to evaluate the role of enterocyte TLR4 signaling in the pathogenesis of NEC using an experimental model that we have established in our laboratory (18). To do so, we inhibited TLR4 signaling in enterocytes by expressing dominant negative TLR4 bearing the inhibitory P712H mutation (7). The expression of a TLR4-mutant adenovirus was found to inhibit TLR4 signaling, as LPS caused an increase in the phosphorylation of p38-MAPK in IEC-6 cells that had been infected with wild-type TLR4 but not mutant TLR4, and mutant GFP-TLR4 prevented the LPS-induced translocation of NF-κB in murine embryonic fibroblasts whereas wild-type GFP-TLR4 did not (data not shown). When administered by enteral gavage to 10-day-old Swiss Webster mice, GFP was detected by RT-PCR in intestinal mucosal scrapings at high copy, but not in lung or liver (data not shown). Importantly, the administration of adenoviral GFP, GFP-wild-type TLR4, and GFP-dominant negative TLR4 to mice that had been induced to develop NEC resulted in GFP expression that was confined predominantly in enterocytes (Fig. 2, *B–D*), suggesting the possibility that this approach could be used to affect enterocyte TLR4-mediated signaling and potentially the severity of NEC in vivo. Strikingly, the severity of NEC was significantly reduced in animals that were administered mutant TLR4 compared with animals that were administered either adenoviral GFP or adenoviral GFP-wild-type TLR4 as gauged by histology (Fig. 2, *H* vs *F* and *G*), the gross appearance of the intestine (Fig. 2, *L* vs *J* and *K*), and the expression of IL-6 within the intestinal mucosa (Fig. 2*M*). Of note, the decrease in the severity of NEC that was observed in mice that had been administered GFP-mutant TLR4 was associated with an increase in the intestinal expression of TLR9, as compared with mice administered wild-type TLR4 or GFP alone (Fig. 2*N*). Administration of dominant negative TLR4 significantly reduced the severity of experimental NEC as determined by examination of the intestinal microarchitecture, as compared with animals that were induced to develop NEC and administered GFP alone or wild-type TLR4 (Fig. 2*O*). Taken together, these findings suggest that TLR4 signaling in enterocytes plays a role in the pathogenesis of intestinal inflammation in an animal model of NEC and raise the possibility that that a relationship between TLR4 and TLR9 signaling may contribute to the development of this disease.

TLR9 activation reduces TLR4 signaling in enterocytes in vitro and in vivo

We next sought to assess the effects of TLR9 activation on the extent of TLR4 signaling using three independent measures. As is shown in Fig. 3, LPS caused the translocation of the p65 subunit of the NF-κB complex from the cytoplasm into the nucleus in

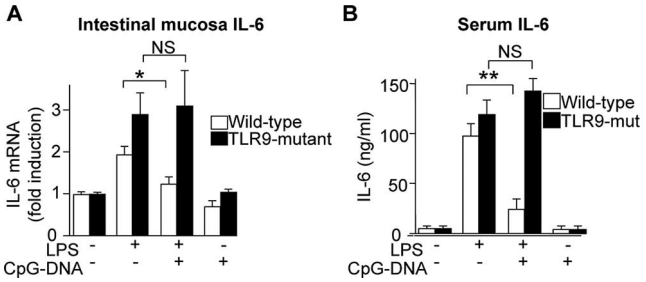

FIGURE 5. CpG-DNA attenuates TLR4-mediated IL-6 expression in the intestine and release into the serum. *A*, Quantitative RT-PCR of ileal mucosal scrapings showing the expression of IL-6 in C57BL/6 (open bars) and TLR9-mutant mice (closed bars) that had been injected with LPS (5 mg/kg) and/or CpG-DNA (1 mg/kg) 3 h earlier. *B*, Measurement of IL-6 in serum by ELISA of C57BL/6 (open bars) and TLR9 mutant mice (filled bars) injected with LPS and/or CpG-DNA as in *A*. Shown are mean and SEM of four separate experiments with five animals per group; *, $p = 0.025$; **, $p = 0.006$.

IEC-6 cells (Fig. 3*B*, filled bars), cells that express both TLR4 and TLR9 (data not shown). By contrast, activation of TLR9 with CpG-DNA significantly reduced the extent of NF-κB translocation, whereas treatment of IEC-6 cells with CpG-DNA alone had little effect on the extent of NF-κB translocation. There was no effect on TLR4-mediated NF-κB translocation by treatment with GpC-DNA, an oligonucleotide that has the CG motifs switched to GC motifs, rendering this molecule incapable of signaling through TLR9. Knockdown of TLR9 with siRNA (confirmed by RT-PCR; Fig. 3*A*) resulted in a loss of the effects of CpG-DNA on TLR4-mediated NF-κB translocation (Fig. 3*B*, open bars). In additional control experiments, CpG-DNA inhibited TLR4-mediated NF-κB translocation in IEC-6 cells that had been treated with scrambled (control) siRNA (Fig. 3*B*, checkered bars).

TLR9 activation in IEC-6 cells with CpG-DNA also reduced the LPS-mediated increase in phosphorylation of p38 and phospho-ERK (Fig. 4*A*), two early downstream molecules important in TLR4 signaling (25), and attenuated the LPS-induced increase in

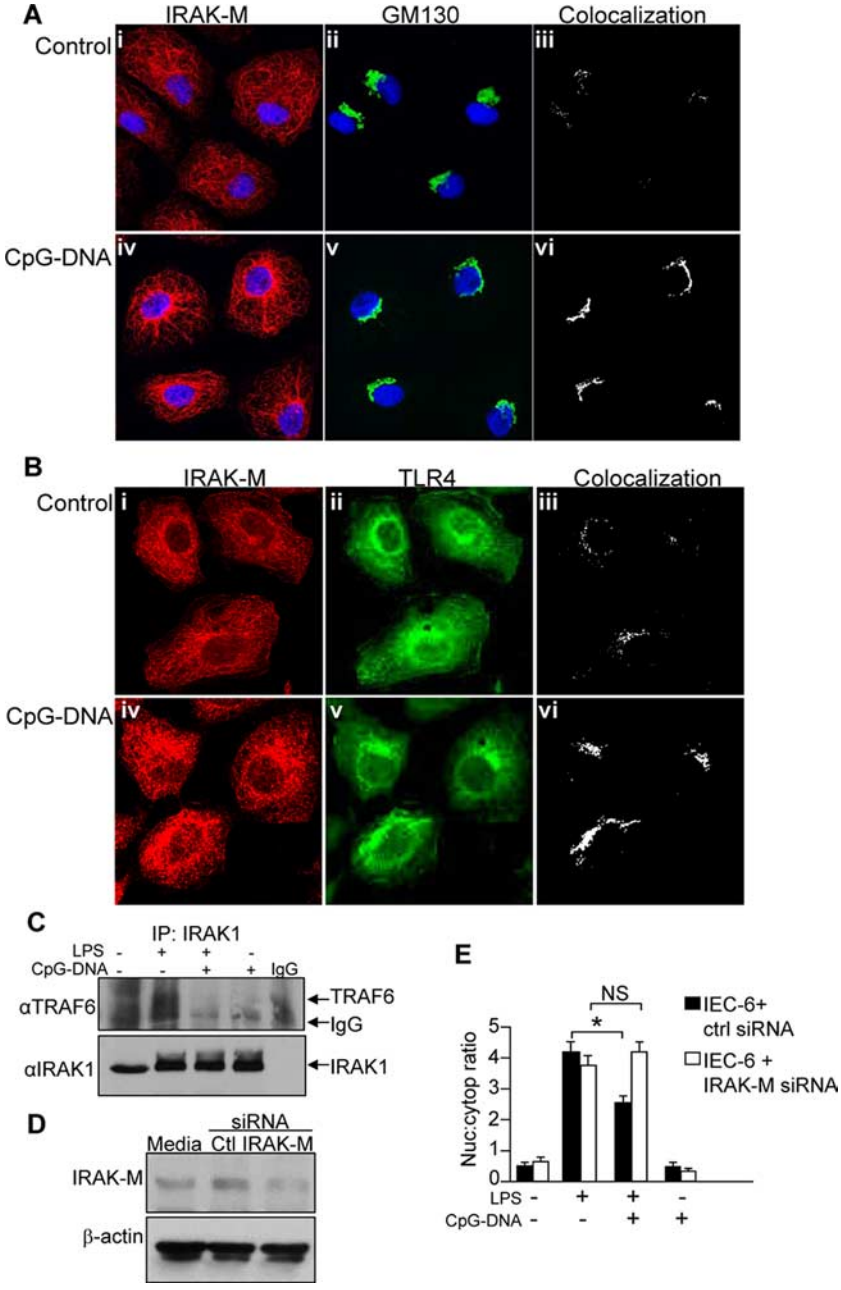

FIGURE 6. CpG-DNA causes the redistribution of IRAK-M to the Golgi apparatus and the inhibition of TLR4 signaling in enterocytes. *A*, Representative confocal micrographs of IEC-6 cells showing the localization of IRAK-M (Cy3; red) and the Golgi marker GM130 (Alexa Fluor 488; green), as well as the nuclear marker Draq-5 (blue) in the absence (*i–iii*) or presence (*iv–vi*) of CpG-DNA (1 μM for 30 min). The extent of colocalization of IRAK-M and GM130 is shown (*iii* and *vi*). Results are representative of five separate experiments. *B*, Representative confocal micrographs of IEC-6 cells showing the localization of IRAK-M (Cy3; red) and TLR4 (Alexa Fluor 488; green) in the absence (*i–iii*) or presence (*iv–vi*) of CpG-DNA (1 μM for 30 min). The extent of colocalization of IRAK-M and TLR4 is shown (*iii* and *vi*). Results are representative of five separate experiments. *C*, In vitro interaction of IRAK1 and TRAF6 in IEC-6 cells as shown by immunoprecipitation (IP). Cells (1×10^6) were processed in each group. *Upper blot* represents SDS-PAGE showing the expression of TRAF6 in IEC-6 cells that were either untreated or treated with LPS (50 μg/ml) and/or CpG-DNA (1 μM for 2.5 min) as indicated and described in *Materials and Methods*. IgG represents whole cell lysates immunoprecipitated with irrelevant IgG. Blots were stripped and reprobed for the expression of IRAK1. The location of TRAF6, IgG, and IRAK1 are indicated by arrows. αTRAF6, Anti-TRAF6 Ab; αIRAK1, anti-IRAK1 Ab. *D*, SDS-PAGE of IEC-6 cells that had been either untreated (Media) or treated with siRNA against no known target (Ctl, Control) or with siRNA against IRAK-M (IRAK-M; 100 nM). *E*, The effect of inhibition of IRAK-M on the extent of CpG-DNA on TLR4-induced NF-κB translocation. Graph shows the mean and SEM of the relative expression of the p65 subunit of NF-κB in nontransfected IEC-6 cells (filled bars) and IEC-6 cells that had been transfected with siRNA to IRAK-M (open bars) in the presence of LPS (50 μg/ml for 1 h) and/or CpG-DNA (1 μM) as indicated. *, $p < 0.001$ by ANOVA of three separate experiments.

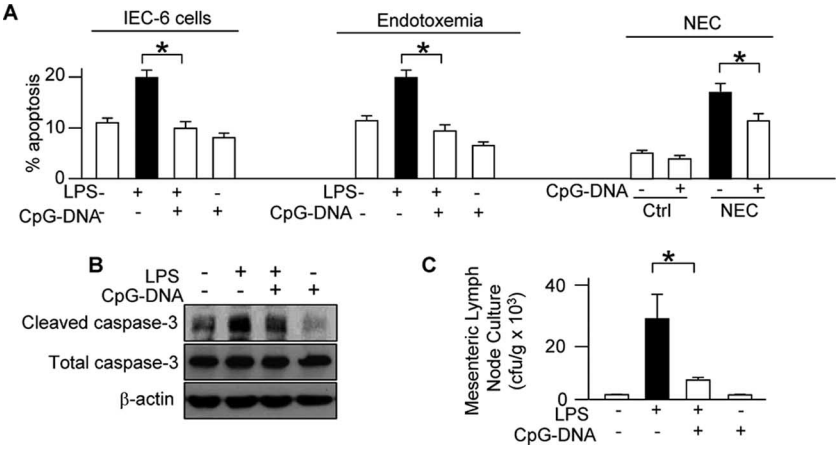

FIGURE 7. CpG-DNA attenuates TLR4-mediated apoptosis in enterocytes in vitro and in vivo and reduces bacterial translocation across the intestinal barrier. *A*, Quantification of confocal micrographs of IEC-6 cells that were untreated or treated with LPS (50 μg/ml for 18h) in the absence or presence of CpG-DNA (1 μM) or treated with CpG-DNA (1 μM) alone. Results are representative of over four separate experiments with >50 cells per field. Quantification of confocal micrographs of terminal ilea of Swiss Webster mice that had been injected with either saline, LPS (5 mg/kg for 14 h) in the presence or absence of CpG-DNA (1 mg/kg) or CpG-DNA alone (1 mg/kg, 14 h). Results are representative of over four separate experiments with at least five mice per experiment. Shown also is the quantification of apoptosis by measuring caspase 3 staining in the terminal ilea of Swiss Webster mice that were either breast fed or were induced to develop NEC using the combination of gavage feeds and hypoxia and then injected with either saline or CpG-DNA. Results are representative of over four separate experiments with at least five mice per experiment. *, $p < 0.001$ by ANOVA. Ctrl, Control. *B*, SDS-PAGE showing cleaved caspase-3 in IEC-6 cells treated with LPS and/or CpG-DNA as indicated and then stripped and reprobed for total caspase-3 and β-actin. Results are representative of three separate experiments. *C*, Quantification of bacterial growth from mesenteric lymph nodes of mice under the conditions indicated. Shown are mean ± SEM; *, $p < 0.005$.

the expression of IL-6 (Fig. 4*B*). In these studies, LPS and CpG-DNA are added concomitantly. Treatment of IEC-6 cells with CpG-DNA alone did not change the phosphorylation of these MAPKs or IL-6 release, demonstrating that CpG-DNA itself has little "activating" effect on enterocytes. There was no effect on LPS-mediated signaling of the inactive oligonucleotide GpC-DNA (not shown). Although CpG-DNA attenuated LPS signaling in enterocytes, there was no effect of CpG-DNA on TLR4 signaling in macrophages as manifested by a lack of effect of CpG-DNA on the LPS-mediated increase in phosphorylation of ERK (Fig. 4*C*) or expression of IL-6 (Fig. 4*D*), consistent with previous reports (26).

Having shown that TLR9 activation limits TLR4 signaling in enterocytes in vitro, we next sought to evaluate the effects of TLR9 activation on TLR4 signaling in vivo. Injection of C57BL/6 mice with LPS led to an increase in the expression of IL-6 in the intestinal mucosa at 3 h (Fig. 5*A*, open bars), as well as a marked increase in the release of IL-6 into the serum at 3 h (Fig. 5*B*, open bars), both of which were significantly reduced upon injection of mice with CpG-DNA. Injection of TLR9-mutant mice with CpG-DNA did not reduce the observed LPS-induced increase in IL-6 expression, confirming the specificity of CpG-DNA for TLR9 in these studies (Fig. 5, *A* and *B*, filled bars). Taken together, these findings illustrate that CpG-DNA activation of TLR9 attenuates TLR4 signaling in enterocytes in vitro and within the intestinal mucosa in vivo.

CpG-DNA causes the redistribution of IRAK-M to the Golgi apparatus and the inhibition of TLR4 signaling in enterocytes

In the next series of experiments, we sought to determine the potential mechanisms by which TLR9 activation with CpG-DNA could attenuate LPS signaling in enterocytes. Previous authors have shown that IRAK-M exerts a negative regulatory role on TLR4 signaling in part by inhibiting the phosphorylation of IRAK4, which blocks the interaction of the critical downstream mediator IRAK1 with TRAF6 (27). It has also been demonstrated that TLR4 signaling within enterocytes occurs within the Golgi apparatus in a mechanism that involves the uptake and Golgi-specific transport of LPS (28). We therefore next sought to investigate the possibility that CpG-DNA could inhibit TLR4 signaling through effects on IRAK-M and whether the trafficking of IRAK-M to the Golgi was involved. Exposure of IEC-6 cells to CpG-DNA for 30 min led to a marked redistribution of IRAK-M from the cytoplasm (Fig. 6*A*, *i–iii*) to the Golgi apparatus (Fig. 6*A*, *iv–vi*). Treatment of enterocytes with CpG-DNA also caused IRAK-M to become colocalized with TLR4 within this perinuclear compartment (Fig. 6*B*, *i–iii* vs *iv–vi*). These findings suggest that CpG-DNA causes a relocation of the inhibitory molecule IRAK-M to the TLR4-containing compartment in enterocytes. In control experiments, CpG-DNA did not cause TLR4 or IRAK-M to become colocalized with the lysosomal marker LAMP-2 or the endoplasmic reticulum marker calnexin, confirming the specificity of the effect.

To further assess whether IRAK-M may mediate the inhibitory effects of CpG-DNA on TLR4 signaling, LPS was found to cause the rapid coimmunoprecipitation of IRAK1 with TRAF6 in IEC-6 cells that was decreased upon stimulation with CpG-DNA (Fig. 6*C*). This finding is suggestive of a role for IRAK-M, given that IRAK-M activity is known to decrease IRAK-1 and TRAF6 signaling (27). To investigate the requirement of IRAK-M for CpG-DNA activity on TLR4 signaling in enterocytes directly, the expression of IRAK-M was inhibited in IEC-6 cells using specific siRNA (as shown in Fig. 6*D*, we achieved ~50% protein knockdown). As shown in Fig. 6*E*, the inhibition of IRAK-M abrogated the previously observed effects of CpG-DNA on TLR4-mediated NF-κB nuclear translocation (Fig. 6*E*, open bars). No such abrogation was observed in cells treated with negative control siRNA (Fig. 6*E*, filled bars). Taken together, these findings indicate an important role for IRAK-M in mediating the inhibitory effects of CpG-DNA on TLR4 signaling in enterocytes.

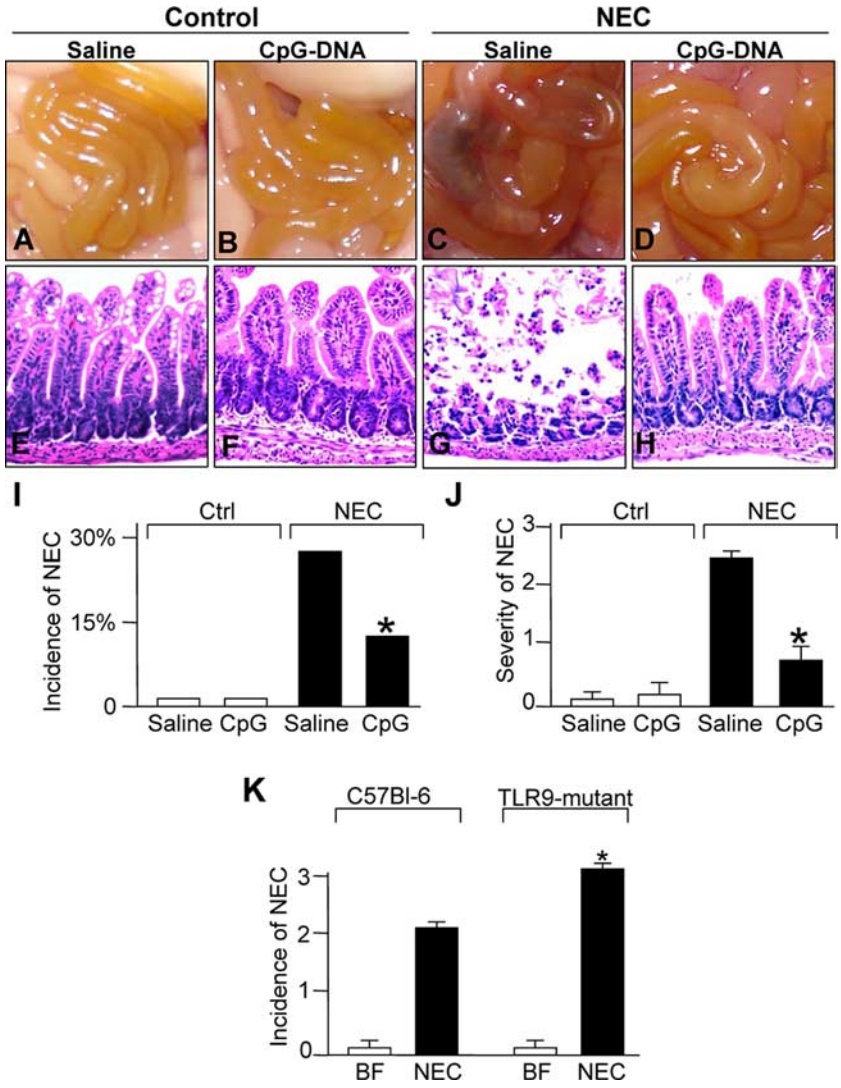

FIGURE 8. CpG-DNA activation of TLR9 reduces the severity of experimental NEC. *A–H*, Representative micrographs showing the gross intestinal morphology (*A–D*) and histopathology (*E–H*) of 10-day-old Swiss Webster mice that were either breast fed (*A* and *B* and *E* and *F*) or induced to develop NEC using the combination of hypoxia and formula gavage (*C* and *D* and *G* and *H*) over 4 days, with twice daily injections with saline or CpG-DNA (1 mg/kg) as indicated. Results are representative of five separate experiments with >15 animals per group. *I* and *J*, Quantification of the incidence (*I*) and severity (*J*) of NEC in breast fed (Ctrl, Control) or formula fed/hypoxia animals (NEC) upon injection with either saline or CpG-DNA. *, $p < 0.05$ by χ^2 analysis vs saline-treated animals with NEC; results are representative of five separate experiments with up to nine mice per group. *K*, Severity of experimental NEC in TLR9-mutant mice (strain CpG1) as compared with their wild-type counterparts (strain C57BL-6) based upon pathological analysis of the terminal ileum. BF, Breast fed. *, $p < 0.05$ vs NEC in wild-type mice by ANOVA. Results are representative of three separate experiments.

CpG-DNA attenuates TLR4-mediated apoptosis in enterocytes in vitro and in vivo and reduces bacterial translocation across the intestinal barrier

Having shown that TLR9 activation with CpG-DNA inhibits TLR4 signaling, we next assessed the physiological effects on intestinal inflammation. We have recently shown that activation of TLR4 in enterocytes initiates apoptosis and plays a key role in the translocation of enteric bacteria across the intestinal barrier (8, 10). We therefore next evaluated whether CpG-DNA affected TLR4-mediated enterocyte apoptosis and the extent of bacterial translocation. As shown in Fig. 7, CpG-DNA significantly attenuated the LPS-induced increase in apoptosis of IEC-6 cells as revealed by the expression of the apoptosis marker cleaved caspase-3 by confocal microscopy (see quantification, Fig. 7*A*) and SDS-PAGE (Fig. 7*B*). This effect was also noted in vivo, as systemic administration of CpG-DNA to mice that also received LPS led to a reduction in the extent of apoptosis of enterocytes in the intestinal mucosa compared with mice that received LPS alone (Fig. 7*A*). CpG-DNA also reduced the extent of LPS-induced bacterial translocation across the intestinal barrier into mesenteric lymph nodes, liver, and spleen (Fig. 7*C*) as compared with the extent of bacterial translocation occurring in animals receiving LPS alone (Fig. 7*C*, *filled bars*), illustrating the physiologic significance of the CpG-DNA mediated TLR4 inhibition.

We have recently shown that NEC is characterized by the development of TLR4-dependent enterocyte apoptosis (8). Importantly, CpG-DNA caused a striking reduction in the extent of enterocyte apoptosis in the ileum of mice that were subjected to a model of experimental NEC as compared with mice administered saline (see quantification, Fig. 7*C*). Injection of mice with CpG-DNA alone did not increase the rate of enterocyte apoptosis compared with untreated animals (Fig. 7*C*). Taken together, these findings indicate that the inhibitory effects of CpG-DNA on TLR4 signaling in enterocytes leads to a reduction in enterocyte apoptosis during endotoxemia and NEC and to a subsequent protection from LPS-induced bacterial translocation across the intestinal barrier.

CpG-DNA activation of TLR9 reduces the incidence of experimental NEC

In the final series of experiments, we sought to determine whether treatment of mice with CpG-DNA would lead to a reduction in the incidence of experimental NEC, a disease that we have shown to be characterized by exaggerated TLR4 signaling and bacterial translocation (8). As shown in Fig. 8, the administration of CpG-DNA caused a striking reduction in the incidence of moderate to severe NEC in Swiss Webster mice, as well as a decrease in the severity of NEC as manifest by examination of the presence of

gross intestinal inflammation and necrosis (Fig. 8, *C* vs *D*), as well as a preservation of ileal microarchitecture (Fig. 8, *G* vs *H*; quantifications, *I* and *J*). In further support of a protective role of TLR9 signaling in the intestine, the induction of experimental NEC in TLR9-mutant mice resulted in a significant increase in disease severity as compared with wild-type C57BL/6 counterparts (Fig. 8*K*). Taken together, these findings suggest a critical role for the balance between TLR4 and TLR9 signaling in the development of NEC and, more specifically, demonstrate that the activation of TLR9 with CpG-DNA reduces the incidence of this newborn intestinal inflammatory disorder.

Discussion

In the current work we provide evidence that the expressions of TLR4 and TLR9 within the developing intestine are reciprocally related, i.e., the expression levels of TLR4 are increased at time points during which TLR9 levels are decreased. We further provide evidence that the unexpected exposure of the developing intestine to endotoxin leads to the expression of the proinflammatory molecules IL-6 and inducible NO synthase within the intestinal mucosa in a pattern that appeared to correlate directly with the expression of TLR4 and inversely with the expression of TLR9, i.e., higher toward the end of gestation when TLR4 expression levels are high with respect to TLR9. These findings suggest that under conditions in which TLR4 expression is high, as may occur in the premature infant, exposure to endotoxin may lead to release of inflammatory mediators and the development of intestinal inflammation. In the context of the pathogenesis of NEC, a septic condition that is confined to the premature population, these findings provide insights into the possibility that the prematurely born infant may be at risk for the development of NEC in part due to the persistently elevated, functional TLR4 in the absence of counter-regulatory TLR9.

The current findings raise the question as to why the expression levels of TLR4 are elevated in the sterile environment of the developing intestine toward the end of gestation. One possibility is that TLR4 may be a receptor for molecules other than LPS that may be present during the microenvironment of the developing intestine. In this regard, TLR4 has been shown to signal in response to heat shock protein 70, a chaperone protein that has a role in the maintenance of the integrity of the intestinal mucosa (29–31). TLR4 has also recently been shown to respond to the cytosolic protein HMGB1 (high molecular group B protein 1), a molecule that is released from damaged cells and may provide a "stress signal" to the host (32). Moreover, TLR4 has also been shown to be a receptor for matrix proteins including fibronectin (33), hyaluronic acid (34), and heparin sulfate (35), molecules that could conceivably play a role in intestinal organogenesis as has been recently demonstrated (36). It remains to be seen, of course, whether the TLR4 that is expressed in the developing intestine is able to respond to any of these stimuli. Similarly, the mechanisms by which TLR9 expression is decreased in the setting of NEC remain to be fully elucidated. In this regard, one could speculate that shared transcription factors acting on the promoter regions of TLR4 and TLR9 may play a role in their reciprocal expression, and/or that the relative roles of the ubiquitin-proteosome pathway may modulate the relative expression of TLR9 and TLR4 in the intestinal mucosa during development and during conditions of injury. We now speculate that the expression of TLR4 and TLR9 within the developing intestine fulfills a role that is independent from its postnatal role in innate immunity. However, when the premature intestine in which the expression of TLR4 remains elevated with respect to TLR9 is colonized with bacteria (37), the subsequent release of proinflammatory molecules places the host at risk of the development of intestinal inflammation and the subsequent mucosal injury that characterizes NEC.

We further provide evidence that activation of TLR9 with CpG-DNA limits TLR4 signaling in enterocytes both in vitro and in vivo and reduces the severity and extent of experimental NEC. The importance of TLR4 activation by LPS to the pathogenesis of NEC is highlighted by previous work from Caplan and colleagues (11) and by work from our group demonstrating that TLR4 plays a critical role in the translocation of Gram negative bacteria across the intestine (10) while also leading to the development of intestinal injury through increased enterocyte apoptosis and reduced mucosal repair through the inhibition of enterocyte proliferation and enterocyte migration in NEC (8). The importance of TLR4 signaling in enterocytes, as opposed to nonepithelial cells, in the pathogenesis of NEC is highlighted by the decrease in the incidence of NEC that was observed in mice that were found to express mutant TLR4 in their enterocytes as opposed to those receiving wild-type virus or GFP alone. These findings raise attention to the study of enterocyte TLR4 signaling in the pathogenesis of NEC and the to the effects of TLR9 on this process. In exerting a protective effect on the intestine in NEC, CpG-DNA was found to reduce the extent of enterocyte apoptosis and the degree of bacterial translocation across the intestinal barrier (Fig. 7), a reflection that the integrity of the intestinal barrier had been maintained. It is noteworthy that CpG-DNA was not found to reduce the inflammatory response to LPS in isolated macrophages (Fig. 4), a finding consistent with previous studies that identify CpG-DNA as an "activator" rather than an "inhibitor" of myeloid cells (38). Given that the net effect of CpG-DNA was to reduce the overall development of systemic inflammation in the current model of NEC (Fig. 8), these findings raise the exciting possibility that administration of CpG-DNA may exert a relative intestinal-specific effect without causing broad myeloid cell immunosuppression.

Although this is the first instance in which CpG-DNA has been shown to limit inflammation and bacterial translocation across the small intestine, CpG-DNA has been shown to reduce the severity of colitis (15, 39, 40); it should be noted though that Obermeier et al. also showed that CpG-DNA can exacerbate experimental colitis through activation of the Th1 arm of the immune system (41, 42). The current work extends these observations by revealing that the protective effects of CpG-DNA in enterocytes occur via the inhibitory kinase IRAK-M and that CpG-DNA causes a redistribution of the inhibitory kinase IRAK-M to a subcellular region within the Golgi apparatus (Fig. 7), the location at which TLR4 is known to respond to LPS in enterocytes (43). The mobilization of IRAK-M to the site of TLR4 signaling would be expected to inhibit the association of IRAK1 and TRAF6 and block the downstream activation of NF-κB, as we now observe, whereas the selective inhibition of IRAK-M prevented the inhibitory effects of CpG-DNA on TLR4 signaling in enterocytes, confirming the importance of IRAK-M in mediating the effects of TLR9 activation on TLR4 signaling (Fig. 6). IRAK-M has been shown to inhibit TLR4 signaling in immune cells, although in such cases the effects are thought to require up to 24 h to occur and to involve an increase in IRAK-M expression (27, 44). The prolonged time required for an increase in IRAK-M expression makes it unlikely that changes in IRAK-M expression could account for the protective effects of TLR9, which we observe to occur within 30 min of exposure (Fig. 4). However, alterations in the trafficking of IRAK-M could provide such an explanation and, in fact, we now observe that CpG-DNA causes a rapid redistribution of IRAK-M so that it becomes colocalized with TLR4 within the Golgi (Fig. 6). The mechanism by which CpG-DNA leads to a redistribution of TLR4 within the

cell remains unclear, although the recent finding that the endoplasmic reticulum protein UNC93B1 regulates the trafficking of TLRs within dendritic cells (45) suggests that similar classes of proteins may play a role in regulating the redistribution of IRAK-M in response to CpG-DNA. It should be pointed out that the expression of IRAK-M was initially considered to be restricted to macrophages (46), although recent studies have shown IRAK-M to be expressed in biliary epithelial cells also (47), and we now describe its expression within enterocytes, suggesting the broader role of IRAK-M in regulating TLR4 signaling in various tissues. Also, although the current studies provide evidence in support of the importance of IRAK-M in mediating the effects of TLR9 activation on TLR4 signaling, we cannot exclude a potential role of other endogenous molecules that have been shown to play important roles in limiting TLR4 responsiveness, including A20 (48), FADD (49), TOLLIP (50) or SHIP (51) or indeed the possibility that TLR9 could trigger the release of type I IFN, which has been shown to exert an anti-inflammatory function in experimental colitis (52).

The current finding that CpG-DNA administration decreases the severity of NEC could provide insights into recent advances in the expanding field of probiotics as it relates to protection from NEC. Two recent randomized controlled trials have demonstrated that administration of probiotic bacteria can decrease the incidence or severity of NEC (53, 54), and similar results have been observed in animal studies (55). Moreover, Raz and colleagues have shown that TLR9 signaling mediates the anti-inflammatory effects of probiotics in a dextran sodium sulfate model of experimental colitis in mice (39). Based upon the current work, we now propose that the protective effects observed in human NEC that were attained through the administration of probiotics may have been achieved in part through the activation of TLR9 in the human intestine by CpG-DNA contained within the probiotics themselves. Further clinical and laboratory studies will be required to evaluate this possibility further and to determine the relevant safety parameters.

In summary, we now report that the intestinal expression of TLR4 and TLR9 are reciprocally related during development, that TLR4 within the intestine is functionally active, and that TLR9 activation with CpG-DNA can limit TLR4 signaling in enterocytes via a mechanism that requires IRAK-M while preventing the development of NEC by limiting TLR4-induced enterocyte apoptosis and bacterial translocation. These findings broaden our understanding of the relative roles of TLR4 and TLR9 signaling in the development of intestinal inflammation while suggesting the possibility of using the TLR9 ligand CpG-DNA as a therapeutic agent in the management of necrotizing enterocolitis.

Acknowledgments

We gratefully acknowledge the gift from Dr. Bruce Beutler, The Scripps Research Institute, for the generous provision of TLR9-mutant mice, and Dr. Marcus Malek, University of Pittsburgh, for technical assistance with the uterine injection studies.

Disclosures

The authors have no financial conflict of interest.

References

1. Blakely, M. L., K. P. Lally, S. McDonald, R. L. Brown, D. C. Barnhart, R. R. Ricketts, W. R. Thompson, L. R. Scherer, M. D. Klein, R. W. Letton, et al. 2005. Postoperative outcomes of extremely low birth-weight infants with necrotizing enterocolitis or isolated intestinal perforation: a prospective cohort study by the NICHD Neonatal Research Network. *Ann. Surg.* 241: 984–989; discussion 989–994.
2. Lin, P. W., and B. J. Stoll. 2006. Necrotising enterocolitis. *Lancet* 368: 1271–1283.
3. Grave, G. D., S. Nelson, W. A. Walker, R. L. Moss, B. Dvorak, F. A. Hamilton, R. Higgins, and T. N. Raju. 2007. New therapies and preventive approaches for necrotizing enterocolitis: report of a research planning workshop. *Pediatr. Res.* 62: 510–514.
4. Hackam, D. J., J. S. Upperman, A. Grishin, and H. R. Ford. 2005. Disordered enterocyte signaling and intestinal barrier dysfunction in the pathogenesis of necrotizing enterocolitis. *Semin. Pediatr. Surg.* 14: 49–57.
5. Miyake, K. 2004. Innate recognition of lipopolysaccharide by Toll-like receptor 4–MD-2. *Trends Microbiol.* 12: 186–192.
6. Lotz, M., D. Gutle, S. Walther, S. Menard, C. Bogdan, and M. W. Hornef. 2006. Postnatal acquisition of endotoxin tolerance in intestinal epithelial cells. *J. Exp. Med.* 203: 973–984.
7. Poltorak, A., X. He, I. Smirnova, M. Y. Liu, C. Van Huffel, X. Du, D. Birdwell, E. Alejos, M. Silva, C. Galanos, et al. 1998. Defective LPS signaling in C3H/HeJ and C57BL/10ScCr mice: mutations in Tlr4 gene. *Science* 282: 2085–2088.
8. Leaphart, C. L., J. Cavallo, S. C. Gribar, S. Cetin, J. Li, M. F. Branca, T. D. Dubowski, C. P. Sodhi, and D. J. Hackam. 2007. A critical role for TLR4 in the pathogenesis of necrotizing enterocolitis by modulating intestinal injury and repair. *J. Immunol.* 179: 4808–4820.
9. Forsythe, R. M., D. Z. Xu, Q. Lu, and E. A. Deitch. 2002. Lipopolysaccharide-induced enterocyte-derived nitric oxide induces intestinal monolayer permeability in an autocrine fashion. *Shock* 17: 180–184.
10. Neal, M. D., C. Leaphart, R. Levy, J. Prince, T. R. Billiar, S. Watkins, J. Li, S. Cetin, H. Ford, A. Schreiber, and D. J. Hackam. 2006. Enterocyte TLR4 mediates phagocytosis and translocation of bacteria across the intestinal barrier. *J. Immunol.* 176: 3070–3079.
11. Jilling, T., D. Simon, J. Lu, F. J. Meng, D. Li, R. Schy, R. B. Thomson, A. Soliman, M. Arditi, and M. S. Caplan. 2006. The roles of bacteria and TLR4 in rat and murine models of necrotizing enterocolitis. *J. Immunol.* 177: 3273–3282.
12. Hemmi, H., O. Takeuchi, T. Kawai, T. Kaisho, S. Sato, H. Sanjo, M. Matsumoto, K. Hoshino, H. Wagner, K. Takeda, and S. Akira. 2000. A Toll-like receptor recognizes bacterial DNA. *Nature* 408: 740–745.
13. Takeuchi, O., K. Hoshino, T. Kawai, H. Sanjo, H. Takada, T. Ogawa, K. Takeda, and S. Akira. 1999. Differential roles of TLR2 and TLR4 in recognition of Gram-negative and Gram-positive bacterial cell wall components. *Immunity* 11: 443–451.
14. Ivory, C. P., M. Prystajecky, C. Jobin, and K. Chadee. 2008. Toll-like receptor 9-dependent macrophage activation by *Entamoeba histolytica* DNA. *Infect. Immun.* 76: 289–297.
15. Rachmilewitz, D., F. Karmeli, S. Shteingart, J. Lee, K. Takabayashi, and E. Raz. 2006. Immunostimulatory oligonucleotides inhibit colonic proinflammatory cytokine production in ulcerative colitis. *Inflamm. Bowel Dis.* 12: 339–345.
16. Hackam, D. J., O. D. Rotstein, A. Schreiber, W. Zhang, and S. Grinstein. 1997. Rho is required for the initiation of calcium signaling and phagocytosis by Fcγ receptors in macrophages. *J. Exp. Med.* 186: 955–966.
17. Cetin, S., J. Dunklebarger, J. Li, P. Boyle, O. Ergun, F. Qureshi, H. Ford, J. Upperman, S. Watkins, and D. J. Hackam. 2004. Endotoxin differentially modulates the basolateral and apical sodium/proton exchangers (NHE) in enterocytes. *Surgery* 136: 375–383.
18. Leaphart, C. L., F. Qureshi, S. Cetin, J. Li, T. Dubowski, C. Batey, D. Beer-Stolz, F. Guo, S. A. Murray, and D. J. Hackam. 2007. Interferon-γ inhibits intestinal restitution by preventing gap junction communication between enterocytes. *Gastroenterology* 132: 2395–2411.
19. Cetin, S., H. R. Ford, L. R. Sysko, C. Agarwal, J. Wang, M. D. Neal, C. Baty, G. Apodaca, and D. J. Hackam. 2004. Endotoxin inhibits intestinal epithelial restitution through activation of Rho-GTPase and increased focal adhesions. *J. Biol. Chem.* 279: 24592–24600.
20. Qureshi, F. G., C. L. Leaphart, S. Cetin, L. Jun, A. Grishin, S. Watkins, H. R. Ford, and D. J. Hackam. 2005. Increased expression and function of integrins in enterocytes by endotoxin impairs epithelial restitution. *Gastroenterology* 128: 1012–1022.
21. Nadler, E. P., E. Dickinson, A. Knisely, X. R. Zhang, P. Boyle, D. Beer-Stolz, S. C. Watkins, and H. R. Ford. 2000. Expression of inducible nitric oxide synthase and interleukin-12 in experimental necrotizing enterocolitis. *J. Surg. Res.* 92: 71–77.
22. Feng, J., and G. E. Besner. 2007. Heparin-binding epidermal growth factor-like growth factor promotes enterocyte migration and proliferation in neonatal rats with necrotizing enterocolitis. *J. Pediatr. Surg.* 42: 214–220.
23. Anand, R., S. Gribar, J. Li, J. Kohler, M. Branca, T. Dubowski, C. Sodhi, and D. Hackam. 2007. Hypoxia causes an increase in phagocytosis by macrophages in a HIF-1α-dependent manner. *J. Leukocyte Biol.* 82: 1257–1265.
24. Cetin, S., C. L. Leaphart, J. Li, I. Ischenko, M. Hayman, J. Upperman, R. Zamora, S. Watkins, H. R. Ford, J. Wang, and D. J. Hackam. 2007. Nitric oxide inhibits enterocyte migration through activation of RhoA-GTPase in a SHP-2-dependent manner. *Am. J. Physiol.* 292: G1347–G1358.
25. Guha, M., and N. Mackman. 2001. LPS induction of gene expression in human monocytes. *Cell. Signal.* 13: 85–94.
26. Sester, D. P., K. Stacey, M. J. Sweet, S. J. Beaseley, and D. A. Hume. 1999. The actions of bacterial DNA on murine macrophages. *J. Leukocyte Biol.* 66: 542–548.
27. Kobayashi, K., L. D. Hernandez, J. E. Galan, C. A. J. Janeway, R. Medzhitov, and R. A. Flavell. 2002. IRAK-M is a negative regulator of Toll-like receptor signaling. *Cell* 110: 191–202.
28. Hornef, M. W., B. H. Normark, A. Vandewalle, and S. Normark. 2003. Intracellular recognition of lipopolysaccharide by Toll-like receptor 4 in intestinal epithelial cells. *J. Exp. Med.* 198: 1225–1235.
29. Bulut, Y., E. Faure, L. Thomas, H. Karahashi, K. S. Michelsen, O. Equils, S. G. Morrison, R. P. Morrison, and M. Arditi. 2002. Chlamydial heat shock

protein 60 activates macrophages and endothelial cells through Toll-like receptor 4 and MD2 in a MyD88-dependent pathway. *J. Immunol.* 168: 1435–1440.
30. Vabulas, R. M., P. Ahmad-Nejad, S. Ghose, C. J. Kirschning, R. D. Issels, and H. Wagner. 2002. HSP70 as endogenous stimulus of the Toll/interleukin-1 receptor signal pathway. *J. Biol. Chem.* 277: 15107–15112.
31. Ohashi, K., V. Burkart, S. Flohe, and H. Kolb. 2000. Cutting edge: heat shock protein 60 is a putative endogenous ligand of the toll-like receptor-4 complex. *J. Immunol.* 164: 558–561.
32. Park, J. S., F. Gamboni-Robertson, Q. He, D. Svetkauskaite, J.-Y. Kim, D. Strassheim, J.-W. Sohn, S. Yamada, I. Maruyama, A. Banerjee, et al. 2006. High mobility group box 1 protein interacts with multiple Toll-like receptors. *Am. J. Physiol.* 290: C917–C924.
33. Okamura, Y., M. Watari, E. S. Jerud, D. W. Young, S. T. Ishizaka, J. Rose, J. C. Chow, and J. F. Strauss III. 2001. The extra domain A of fibronectin activates Toll-like receptor 4. *J. Biol. Chem.* 276: 10229–10233.
34. Termeer, C., F. Benedix, J. Sleeman, C. Fieber, U. Voith, T. Ahrens, K. Miyake, M. Freudenberg, C. Galanos, and J. C. Simon. 2002. Oligosaccharides of hyaluronan activate dendritic cells via toll-like receptor 4. *J. Exp. Med.* 195: 99–111.
35. Johnson, G. B., G. J. Brunn, Y. Kodaira, and J. L. Platt. 2002. Receptor-mediated monitoring of tissue well-being via detection of soluble heparan sulfate by Toll-like receptor 4. *J. Immunol.* 168: 5233–5239.
36. Sedita, J., K. Izvolsky, and W. V. Cardoso. 2004. Differential expression of heparan sulfate 6-*O*-sulfotransferase isoforms in the mouse embryo suggests distinctive roles during organogenesis. *Dev. Dyn.* 231: 782–794.
37. Park, H. K., S. S. Shim, S. Y. Kim, J. H. Park, S. E. Park, H. J. Kim, B. C. Kang, and C. M. Kim. 2005. Molecular analysis of colonized bacteria in a human newborn infant gut. *J. Microbiol.* 43: 345–353.
38. Beutler, B., and A. Poltorak. 2001. Sepsis and evolution of the innate immune response. *Crit. Care Med.* 29: S2–6.
39. Rachmilewitz, D., K. Katakura, F. Karmeli, T. Hayashi, C. Reinus, B. Rudensky, S. Akira, K. Takeda, J. Lee, K. Takabayashi, and E. Raz. 2004. Toll-like receptor 9 signaling mediates the anti-inflammatory effects of probiotics in murine experimental colitis. *Gastroenterology* 126: 520–528.
40. Lee, J., J. H. Mo, K. Katakura, I. Alkalay, A. N. Rucker, Y. T. Liu, H. K. Lee, C. Shen, G. Cojocaru, S. Shenouda, et al. 2006. Maintenance of colonic homeostasis by distinctive apical TLR9 signalling in intestinal epithelial cells. *Nat. Cell Biol.* 8: 1327–1336.
41. Obermeier, F., N. Dunger, L. Deml, H. Herfarth, J. Schölmerich, and W. Falk. 2002. CpG motifs of bacterial DNA exacerbate colitis of dextran sulfate sodium-treated mice. *Eur. J. Immunol.* 32: 2084–2092.
42. Obermeier, F., N. Dunger, U. G. Strauch, N. Grunwald, H. Herfarth, J. Schölmerich, and W. Falk. 2003. Contrasting activity of cytosin-guanosin dinucleotide oligonucleotides in mice with experimental colitis. *Clin. Exp. Immunol.* 134: 217–224.
43. Hornef, M. W., T. Frisan, A. Vandewalle, S. Normark, and A. Richter-Dahlfors. 2002. Toll-like receptor 4 resides in the Golgi apparatus and colocalizes with internalized lipopolysaccharide in intestinal epithelial cells. *J. Exp. Med.* 195: 559–570.
44. Deng, J. C., G. Cheng, M. W. Newstead, X. Zeng, K. Kobayashi, R. A. Flavell, and T. J. Standiford. 2006. Sepsis-induced suppression of lung innate immunity is mediated by IRAK-M. *J. Clin. Invest.* 116: 2532–2542.
45. Kim, Y. M., M. Brinkmann, M. E. Paquet, and H. L. Ploegh. 2008. UNC93B1 delivers nucleotide-sensing toll-like receptors to endolysosomes. *Nature* 452: 234–238.
46. Wesche, H., X. Gao, X. Li, C. J. Kirschning, G. R. Stark, and Z. Cao. 1999. IRAK-M is a novel member of the Pelle/interleukin-1 receptor-associated kinase (IRAK) family. *J. Biol. Chem.* 274: 19403–19410.
47. Harada, K., I. K. Sato, Y. Ozaki, and S. Nakanuma. 2006. Endotoxin tolerance in human intrahepatic biliary epithelial cells is induced by upregulation of IRAK-M. *Liver Int.* 26: 935–942.
48. Wullaert, A., L. Verstrepen, S. Van Huffel, M. Adib-Conquy, S. Cornelis, M. Kreike, M. Haegman, K. El Bakkouri, M. Sanders, K. Verhelst, et al. 2007. LIND/ABIN-3 is a novel lipopolysaccharide-inducible inhibitor of NF-κB activation. *J. Biol. Chem.* 282: 81–90.
49. Zhande, R., S. M. Dauphinee, J. A. Thomas, M. Yamamoto, S. Akira, and A. Karsan. 2007. FADD negatively regulates lipopolysaccharide signaling by impairing interleukin-1 receptor-associated kinase 1-MyD88 interaction. *Mol. Cell. Biol.* 27: 7394–7404.
50. Didierlaurent, A., B. Brissoni, D. Velin, N. Aebi, A. Tardivel, E. Käslin, J. C. Sirard, G. Angelov, J. Tschopp, and K. Burns. 2006. Tollip regulates proinflammatory responses to interleukin-1 and lipopolysaccharide. *Mol. Cell. Biol.* 26: 735–742.
51. Fang, H., R. A. Pengal, X. Cao, L. P. Ganesan, M. D. Wewers, C. B. Marsh, and S. Tridandapani. 2004. Lipopolysaccharide-induced macrophage inflammatory response is regulated by SHIP. *J. Immunol.* 173: 360–366.
52. Katakura, K., J. Lee, D. Rachmilewitz, G. Li, L. Eckmann, and E. Raz. 2005. Toll-like receptor 9-induced type I IFN protects mice from experimental colitis. *J. Clin. Invest.* 115: 695–702.
53. Bin-Nun, A., R. Bromiker, M. Wilschanski, M. Kaplan, B. Rudensky, M. Caplan, and C. Hammerman. 2005. Oral probiotics prevent necrotizing enterocolitis in very low birth weight neonates. *J. Pediatr.* 147: 192–196.
54. Lin, H. C., B. H. Su, A. C. Chen, T. W. Lin, C. H. Tsai, T. F. Yeh, and W. Oh. 2005. Oral probiotics reduce the incidence and severity of necrotizing enterocolitis in very low birth weight infants. *Pediatrics* 115: 1–4.
55. Siggers, R. H., J. Siggers, M. T. Thymann, L. Mølbak, T. Leser, B. B. Jensen, and P. T. Sanglid. 2008. Early administration of probiotics alters bacterial colonization and limits diet-induced gut dysfunction and severity of necrotizing enterocolitis in preterm pigs. *J. Nutr.* 138: 1437–1444.